Applied Catalysis B: Environmental 218 (2017) 743–750

Contents lists available at ScienceDirect

Applied Catalysis B: Environmental

journal homepage: www.elsevier.com/locate/apcatb

Palladium-decorated hierarchical titania constructed from the metal-organic frameworks NH_2-MIL-125(Ti) as a robust photocatalyst for hydrogen evolution

Baolin Yan[a,b], Lijuan Zhang[c,d], Zhiyong Tang[c], Mohammad Al-Mamun[c], Huijun Zhao[c], Xintai Su[a,*]

[a] Department of Chemistry, Zhejiang Sci-Tech University, Xiasha Campus, Hangzhou 310018, China
[b] Ministry Key Laboratory of Oil and Gas Fine Chemicals, College of Chemistry and Chemical Engineering, Xinjiang University, Urumqi 830046, China
[c] Centre for Clean Environment and Energy Griffith University Gold Coast Campus, Queensland 4222, Australia
[d] Center for Micro and Nanotechnology, Harbin Institute of Technology, Harbin 150080, China

ARTICLE INFO

Article history:
Received 5 May 2017
Received in revised form 2 July 2017
Accepted 9 July 2017
Available online 11 July 2017

Keywords:
MOFs
NH_2-MIL-125
Hierarchical
Pd/TiO_2
Photocatalytic H_2-production

ABSTRACT

Engineering metal-organic frameworks (MOFs) into hierarchical structured materials is crucial for providing a viable platform to construct efficient catalysts and broaden their applications in energy conversion and photocatalysis. Here, a simple and efficient solid-state pyrolysis of Ti-MOFs (NH_2-MIL-125) sacrificial template combined with a photo-reduction process was developed to construct a series of hierarchical TiO_2 decorated with Pd nanoparticles. The hierarchical TiO_2 inherited the well-defined rounded rectangular submicron-tablet from NH_2-MIL-125 precursor and was constituted of uniform anatase TiO_2 nanoparticles with an average size of 12 nm. Furthermore, the photocatalytic activity for the hydrogen production from water-methanol solution was improved by the optimization of the content of Pd as a cocatalyst, and the maximum was achieved with a Pd loading of 1.5%. The rate of H_2 evolution of 1.5% Pd decorated hierarchical TiO_2 (1.5% Pd/TiO_2) reached to 979.7 $\mu mol\ h^{-1}$ and 112.7 $\mu mol\ h^{-1}$, under UV–vis light and simulated solar light, respectively. This unusual photocatalytic activity may be resulted from the positive synergetic effect of efficient light absorption, promoted separation and migration of photo-induced electron-hole carriers. The work highlights the potential of the MOFs-based hierarchical TiO_2 in the photocatalytic water splitting under solar light.

1. Introduction

Solar photocatalysis in the conversion of photo-energy to clean and renewable hydrogen fuel has spurred the vast amounts of research endeavors for its significant effects on resolving the urgent energy crisis and environmental issue [1,2]. The foremost blueprint for photocatalytic splitting of water into hydrogen was depicted with utilization of TiO_2 semiconductor by Fujishima and Honda in 1972 [3]. From then on, considerable efforts have been dedicated to extending its light-absorption region and improving its photocatalytic performance by doping [4,5], modification [6,7], and constructing a TiO_2-based heterojunction to drive the transfer and separation of the photo-generated charge [8,9]. Besides, since catalytic reaction is mainly taking place at the surface of the catalyst, the structure of the TiO_2 photocatalyst has vital effect on photocatalytic efficiency and a higher surface area facilitates accessibility to the reactants [10]. Therein, engineering TiO_2 into a hierarchical structure with large specific surface area is a satisfactory alternative to provide more exposed active sites and interfaces for photocatalytic reaction. Accordingly, constructing the hierarchical structure of TiO_2 for photocatalysis has received some extensive attention and some progress has been achieved [11]. Primarily, the TiO_2 could be synthesized by solution methods accompanied by self-assembly or templated growth [12,13]. Yet, these routes generally require large quantities of toxic and expensive precursors, surfactants and additional templates to realize the assembly procedure [14]. Thereby, in order to bring it to be a more pragmatic and effective photocatalyst, hierarchical porous TiO_2 with a higher surface area and pore volume produced by a facile way is highly imperative.

Metal-organic frameworks (MOFs) are crystalline functional materials constructed by metallic ions (clusters) and organic linkers [15,16]. They have been intensely exploited in gas storage [17],

* Corresponding author.
E-mail address: suxintai827@163.com (X. Su).

http://dx.doi.org/10.1016/j.apcatb.2017.07.020
0926-3373/

catalysis [18], sensing [19], electrochemical [20,21] and photocatalysis [22], etc., owing to their high porosities and regularity, simultaneously tunable pore structures. In recent years, MOFs have been either explored as sacrificial precursors or templates for highly porous/hollow hierarchical metal oxides prepared by solid state thermal decomposition [23–25]. When they are utilized as photocatalysts, the metal oxides derived from MOFs endow some potential merits, such as high light-harvesting and efficient charge transform that arise from their certain degree of inherited porosity and atomic long-range ordering [26,27].

Until now, the MIL-125 and its derivatives are some of the earliest Ti-containing MOFs [28], and their photocatalytic performances have been evaluated by degradation of organic contaminant [29,30], water splitting [31,32] and CO_2 reduction [33]. However, their photocatalytic activities are greatly restricted by the structural instability which is attributed from the lapsable coordination bonds in the MIL-125. Alternatively, pyrolytic conversion of the MIL-125 into TiO_2 is a promising strategy to improve the stability while preserve the porous structure and high specific surface area. Though the MIL-125 derived hierarchical TiO_2 have been extensively applied in electrochemistry as an electrode material, the MIL-125 derived hierarchical TiO_2 as photocatalyst for water splitting is still rarely reported [34–37]. Particularly, Zhao et al. [38] synthesized TiO_x/C composites by pyrolyzing MIL-125 under a high temperature, which were employed to photo-degradation of methylene blue (MB) in aqueous solution. Besides, based on pyrolytic conversion of the NH_2-MIL-125(Ti) loaded with Au nanoparticles, Au/TiO_2 were prepared and exhibited high photocatalytic activities for CO_2 reduction [39]. Nevertheless, the practical applications of the hierarchical TiO_2 photocatalysts are still limited by their narrow spectral absorption range and high recombination of photo-induced electron-hole pairs. Therefore, heterostructures of the hierarchical TiO_2 with other oxides, sulfides and noble metals including Ag, Au, Pd, and Pt, have been exploited [40–42]. Wherein, coupling noble metal cocatalyst species with the TiO_2 can generate a Schottky junction on the interfacial surface to facilitate charge-transfer processes or increase the amounts of surface reacting sites and enlarge the range of light-response [43].

To the best our knowledge, there are few reports focused on the photocatalytic performance of the hierarchical TiO_2 derived from MOFs precursor. Therefore, it is necessary to systematically study the H_2 production activities of the hierarchical TiO_2 decorated with various noble metals under different irradiation. Herein, we constructed a series of Pd modified hierarchical TiO_2 photocatalysts by a simple solid-state pyrolysis of Ti-MOF (NH_2-MIL-125) sacrificial template combined with a photo-reduction process. The as-obtained Pd/TiO_2 composite photocatalysts demonstrated superior photocatalytic activities towards H_2 evolution compared to pure hierarchical TiO_2 under UV–vis light and simulated solar light. Notably, the optimal amount of Pd on TiO_2 for increasing the photocatalytic activity was 1.5% due to the higher light adsorption, more efficient separation and transfer of the photo-generated charge carriers.

2. Experimental section

2.1. Materials

Tetrapropyl orthotitanate (TPOT; $Ti(OC_3H_7)_4$) and Palladium chloride ($PdCl_2$) were purchased from Aladdin Co., Ltd., China. 2-Amino-benzenedicarboxylic acid ($H_2BDC\text{-}NH_2$; $C_8H_7NO_4$) was purchased from TCI Co. *N*,*N*-dimethylformamide (DMF; $(CH_3)_2NCHO$) was purchased from Alfa Aesar Co. Methanol (CH_3OH) was purchased from Tianjin Zhiyuan Chemical Reagents Co., Ltd.

2.2. Synthesis of NH_2-MIL-125(Ti) precursor

The NH_2-MIL-125(Ti) as a sacrificial template was prepared by a solvothermal method, which was modified from a previous report [44]. Typically, TPOT (0.75 mL, 2.5 mmol) and $H_2BDC\text{-}NH_2$ (0.68 g, 3.75 mmol) were added into a mixed solution of DMF (45.0 mL) and CH_3OH (5.0 mL), followed the mixture was subjected to a 100 of mL Teflon-lined stainless-steel autoclave and heated at 150 °C for 72 h. After being cooled, the obtained yellow suspension of NH_2-MIL-125(Ti) was centrifuged and washed with DMF and CH_3OH three times, respectively.

2.3. Fabrication of Pd/TiO_2

The pristine hierarchical TiO_2 was synthesized by the simple pyrolytic conversion of NH_2-MIL-125(Ti). The as-synthesized NH_2-MIL-125(Ti) was heated to 400 °C at a ramp of 1 °C min^{-1} and maintained at the temperature for 4 h under air. Upon naturally cooling down, pale powder of TiO_2 was obtained. Subsequently, the TiO_2 was modified with a nominal Pd loading amounts of 0.5%, 1.0%, 1.5%, 2.0%, 2.5%, respectively, by a light-reduction process. In each case, 400 mg of TiO_2 was dispersed in 80.0 mL of methanol in a Pyrex glass vessel and corresponding volume of $PdCl_2$ (10 mM, in HCl aqueous solution) were introduced, and then the reactor was sealed and bubbled with Ar gas to eliminate dissolved O_2 in the solution. Afterward, the mixed solution was subject to light-irradiated for 2 h by a 300 W Xe lamp with the range of 320–780 nm and no cut-off was employed. The resultant powder was washed with distilled water and ethanol several times and dried at 60 °C in a vacuum oven. For comparison, the 1.5% Pd/NH_2-MIL-125(Ti) composite was obtained by the same process.

2.4. Characterization

The crystal structure of as-obtained products were characterized by X-ray diffraction (XRD) on Bruker D8 X-ray diffractometer with Cu-Kα radiation (λ = 1.54178 Å) in 2θ ranging from 5° to 80°. Transmission electron microscopy (TEM) and high-resolution TEM (HRTEM) images were carried out on a Tecnai F30 microscope with an accelerating voltage of 100 kV. Field-emission scanning electron microscope (FE-SEM) equipped with Energy Dispersive Spectrometer (EDS) were performed on a Hitachi SU8010 microscope operated at 5 kV. The surface area and porosity analyzer were obtained on a Micromeritics ASAP 2020 physisorption instrument by Brunauer-Emmett-Teller (BET) and Barrett-Joyner-Halender (BJH) method. X-ray photoelectron spectroscopy (XPS) analyses were performed on Thermo Fisher Scientific XPS ESCALAB 250Xi instrument with an Al-Kα (1486.8 eV) X-ray source. Thermogravimetric analysis (TGA) was taken on a thermogravimetric analyzer (Netzsch TGA 409) from ambient to 800 °C with a heating rate of 10 °C min^{-1} under air condition. UV–vis diffuse reflectance spectra (UV-DRS) were measured on a Hitachi spectrophotometer using $BaSO_4$ as a reference. Photoluminescence (PL) spectra of the products were recorded with a fluorescence spectrophotometer (Hitachi F-4500) by using the excited wavelength of 300 nm. The amounts of Pd on the catalysts were determined by using an inductively coupled plasma atomic emission spectroscopy (ICP-AES).

2.5. Photoelectrochemical measurements

The transient photocurrent response and electrochemical impedance spectroscopy (EIS) were performed on a CHI 660D electrochemical workstation (Chenhua Instrument, Shanghai, China), using standard three-electrode system, of which Ag/AgCl and Pt electrodes were served as the counter and reference electrodes, respectively. The working electrodes were prepared as follows:

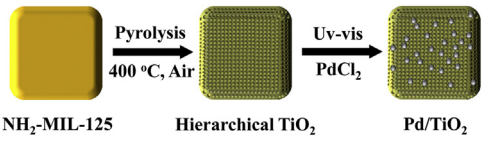

Fig 1. Schematic illustration of the synthesis of the hierarchical Pd/TiO_2 by the MOFs-templated transformation route, combined with photo-reduction process.

5.0 mg of as-synthesized samples was mixed with 1 mL of ethanol and sonicated to form a homogeneous suspension. And then, the suspension was coated onto a 2.5 cm × 1.5 cm F-doped SnO_2-coated glass (FTO glass) electrode with a uniform and similar thickness. Subsequently, the electrode was vacuum dried at 110 °C for 12 h. The electrolyte utilized in the photocurrent and EIS measurement is 0.5 M Na_2SO_4 solution.

2.6. Photocatalytic H_2 evolution measurements

The photocatalytic H_2 generated reactions of the samples were performed in a top irradiation-type photo-reactor (Perfect Light Company, China) connected to a closed gas-circulation system. A 300 W Xe arc lamp (Microsolar 300, λ = 320–780 nm) with or without applying a cut-off filter of AM1.5G was employed to obtain simulated solar light or UV–vis irradiation respectively. In a typical experiment, 20 mg of catalyst was dispersed in 100 mL aqueous solution containing 20 vol% methanol as a sacrificial reagent, without deposition of additional cocatalyst. The suspension was thoroughly evacuated to remove air and ensure that the reaction system was under anaerobic conditions. The procreant gases were analyzed by a gas chromatography equipped with a thermal conductive detector (TCD, 5 Å molecular sieve column) with Ar gas as the carrier gas.

3. Results and discussion

The synthetic procedure of Pd decorated hierarchical porous TiO_2 is demonstrated in Fig. 1. NH_2-MIL-125(Ti) with the formula of $[Ti_8O_8(OH)_4(C_6H_3C_2O_4NH_2)_6]$ were constructed by Ti oxo-clusters and organic linkers. The phase purity and light absorption intensity of the as-synthesized NH_2-MIL-125(Ti) have confirmed by simulated XRD patterns and UV-DRS respectively (Fig. S1), the results were well in accordance with the previous reports [45]. Thus, the NH_2-MIL-125(Ti) could be utilized as an ideal sacrificial precursor and template to synthesize the hierarchical TiO_2, resulting from its simple and economical fabrication process and precisely reproducible. Before converting the NH_2-MIL-125(Ti) precursor to hierarchical porous TiO_2, the BET surface area and pore volume of the precursor were determined by N_2 adsorption-desorption isotherm and Barrett-Joyner-Halenda (BJH) with the value of 947.85 $m^2 g^{-1}$ and 0.276 $cm^3 g^{-1}$ (Fig. S2). The conversion was achieved by the directly solid state pyrolysis of the NH_2-MIL-125(Ti) under constant air at given temperature. The appropriate temperature and heating ramp are critical factors to control the porosity, size and shape for the conversion of TiO_2. Too high temperature make the small particles grow into big ones and the pores/channels in the NH_2-MIL-125(Ti) may be diminished because they interact with each other. Therefore, it is fundamental necessary to investigate the thermal decomposition behavior of the NH_2-MIL-125(Ti) precursor to obtain the porous TiO_2 with a small grain size and moderate BET surface area. As shown in Fig. S3, the first weight loss from 45 °C to 100 °C is attributed to the release of methanol and the second slow weight loss in the 100–300 °C is the removal of DMF molecules and other unreacted organic chemicals adsorbed into NH_2-MIL-125(Ti) pores. The main weight loss is between 300 °C and 570 °C, corresponds to the decomposition

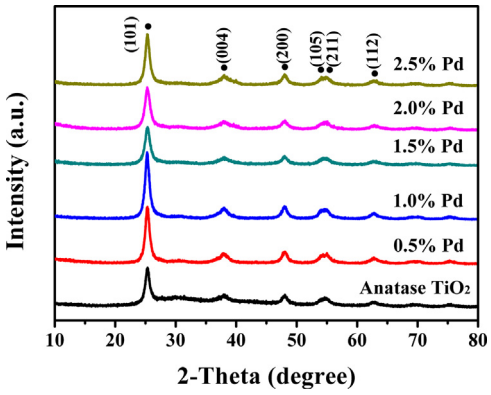

Fig. 2. XRD patterns of pure hierarchical TiO_2 constructed from NH_2-MIL-125(Ti) and the corresponding Pd/TiO_2 with different Pd contents.

of the 2-aminoterephthalic acid frameworks to produce TiO_2. To convert the NH_2-MIL-125(Ti) precursor to TiO_2 completely and maintain its original morphology, a certain degree of high temperature is prerequisite but it should be limited as low as possible. Moreover, the heating rate is as slow as possible. On basis of the TG analysis, we deemed that 400 °C along with a low heating rate of 1 °C min^{-1} is suitable for the pyrolytic conversion of the NH_2-MIL-125(Ti) precursor to TiO_2. Subsequently, the additive Pd was deposited by a photo-reduction process, which is milder and greener, favorably achieves uniform distribution. What's more, the actual amounts of deposited Pd in Pd/TiO_2 were determined by ICP-AES, and almost identical to the amounts of Pd added (Table S1). These testified the photo-reduction approach can effectively adsorb and reduce the Pd nanoparticles in the hierarchical TiO_2 substrate.

The phase structure of the hierarchical TiO_2 constructed from the NH_2-MIL-125(Ti) and corresponding composites of Pd decorated with various amounts were depicted in Fig. 2. After thermolysis, the crystalline phase of NH_2-MIL-125(Ti) precursor has completely vanished and the new phase of anatase TiO_2 (JCPDS no. 21-1272) appeared, indicating that pure TiO_2 phase could be obtained by the current Ti-MOFs-templated transformation route. Meanwhile, the synthesized Pd decorated TiO_2 samples presented XRD patterns similar to pure TiO_2, no significant characteristic peak of Pd could be detected, manifesting high dispersion and small size of Pd nanoparticles on the hierarchical TiO_2 matrix. Moreover, the average crystallites sizes of all the samples were determined from the peaks centered at approximately 25.3°, according to the Scherrer equation. The calculated sizes were mainly 12 nm, which implied that the hierarchical TiO_2 microstructure derived from the Ti-contain MOF was composed of small TiO_2 nanoparticles.

Fig. 3 exhibited cross-sectional SEM images of the NH_2-MIL-125(Ti) precursor (a, b) and the corresponding resultant hierarchical TiO_2 (c, d). The precursor endowed rectangular submicron-tablet architecture with rounded corners. A close observation reveals the precursor was ~1 μm in diameter and ~200 nm in thickness. After pyrolysis conversion, the regular NH_2-MIL-125(Ti) precursor resulted in the well-defined TiO_2 structures, which inherited the structural features of the precursor but has been shrunk and truncated due to the loss of C and H of organic ligands. It is worth mentioning that the surface of the TiO_2 became rougher compared with the NH_2-MIL-125(Ti) precursor, arising from the decomposition of organic ligands and the leaving channels of gas releasing during the thermolysis process. Further, the TEM and HRTEM analysis were employed to observe the detailed structures of the hierarchical TiO_2 derived from Ti-MOF and verify the Pd in the 1.5% Pd/TiO_2 composites. As shown in Fig. 4a and b, the TiO_2 microstructure with a length and width of ~0.5 μm, were composed of closely packed TiO_2 nanoparticles. After modi-

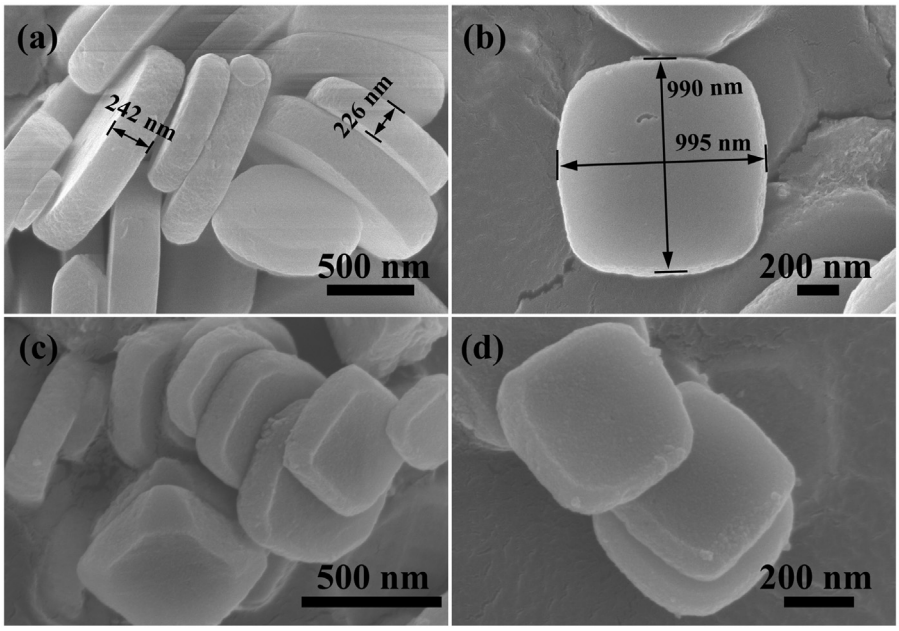

Fig. 3. SEM images of NH_2-MIL-125(Ti) (a, b) and resultant hierarchical TiO_2 (c, d).

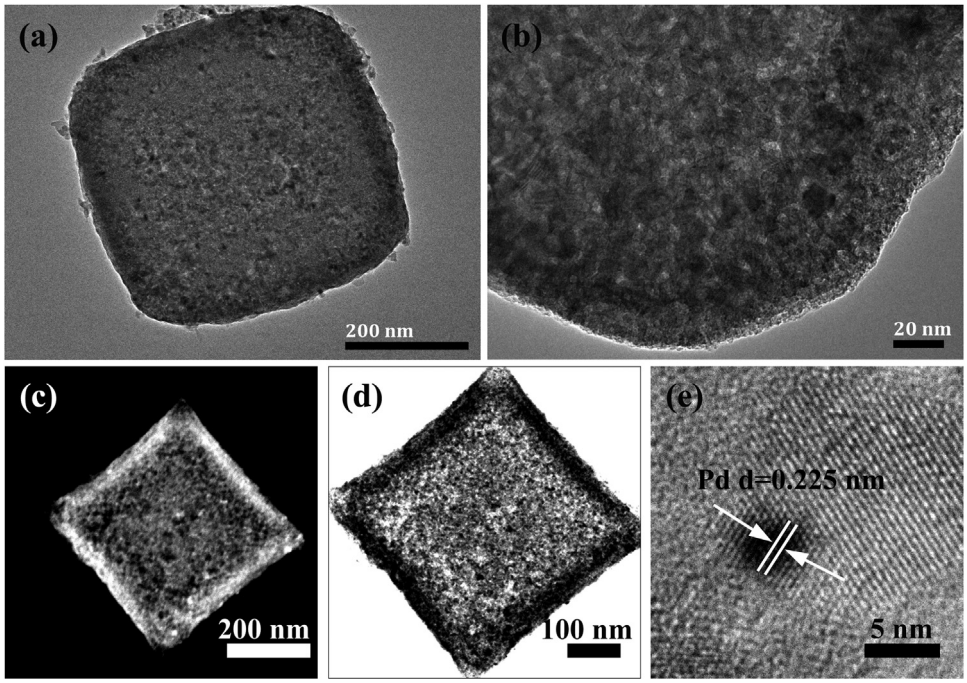

Fig. 4. TEM images of hierarchical TiO_2 (a, b); dark (c), bright field (d) STEM images and (e) HRTEM images of 1.5% Pd/TiO_2.

fied with Pd, the well-defined shape of the hierarchical TiO_2 were preserved (Fig. 4c and d), the dark spherical spots in Fig. 4e represented Pd incorporated in the hierarchical TiO_2, and the lattice fringes with d = 0.225 nm are distinct, which could be ascribed to the (111) planes of Pd nanoparticles. Moreover, the EDS mapping results demonstrated that the Pd was uniformly dispersed in the hierarchical TiO_2 (Fig. S4).

XPS measurement was employed to gain more information about the surface composition and chemical states of TiO_2 and the corresponding decoration of 1.5% Pd (1.5% Pd/TiO_2). As presented in Fig. 5a, an apparent Pd peak was observed in the 1.5% Pd/TiO_2 decoration, which was not emerged in the pure TiO_2, confirming Pd particles were efficiently loaded on the TiO_2 surface. Further, the Pd 3d high-resolution XPS spectra of the 1.5% Pd/TiO_2 showed that the two peaks centered at 340.6 eV (Pd 3d3/2) and 335.4 eV (Pd 3d5/2) are in line with the metallic Pd, while a certain amounts of Pd^{2+} valence state are not to be ignored, owing the doublet peaks at 342.4 eV and 337.4 eV respectively, which may be attributed that the smaller Pd particles with higher activity are accessible to be oxidized under ambient conditions.

To assess the specific surface areas and pore structures of the MOF-constructed hierarchical TiO_2, the N_2 adsorption-desorption measurements were conducted. It is easy to understand that there are no obvious changes on the pore structures of the TiO_2 decorated

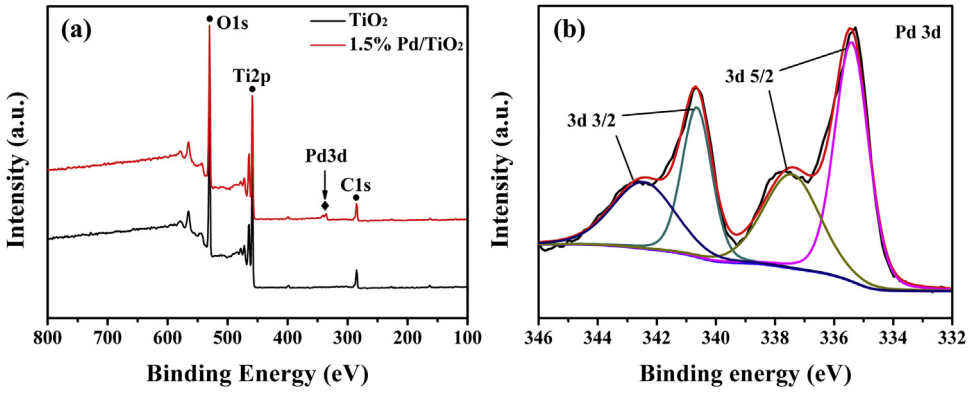

Fig. 5. XPS spectra of hierarchical TiO_2 and 1.5% Pd/TiO_2 (a) full scan survey, (b) Pd 3d.

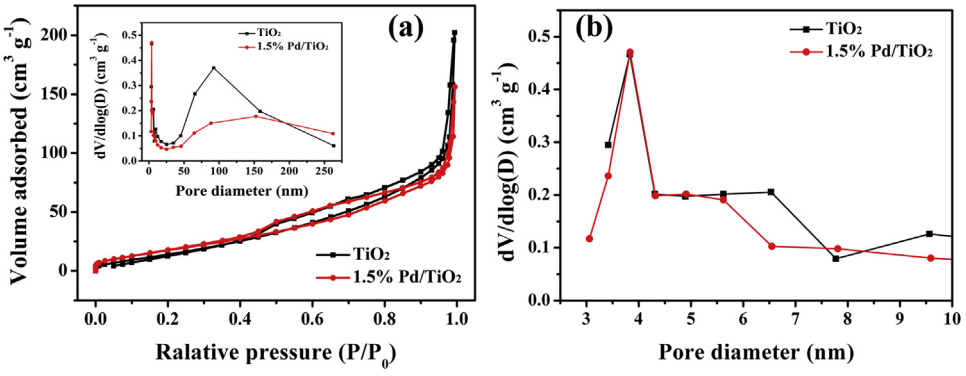

Fig. 6. N_2 adsorption-desorption isotherms of hierarchical TiO_2 and 1.5% Pd/TiO_2 (a); the corresponding BJH desorption pore size distributions curve (inset) and the magnified pore size distributions range from 0 to 10 nm (b).

with additional small amount of Pd. As representatively shown in Fig. 6, the pore size distribution of the pure TiO_2 emerged as hierarchical and bimodal porosity, owing to the mesopores with pore diameters of 3.8 nm, accompanied by the macropores with pore diameters of attained to 90 nm. Such porous structures were inherited from the NH_2-MIL-125(Ti) precursor. The moderate specific surface area of 1.5% Pd/TiO_2 was 86.772 $m^2\ g^{-1}$ with a pore volume of 0.236 $cm^3\ g^{-1}$, which was lower than pure TiO_2 (103.386 $m^2\ g^{-1}$ with a pore volume of 0.326 $cm^3\ g^{-1}$). Moreover, as the Pd amounts increased to 2.5%, the specific surface areas decreased gradually (Supporting Information, Table S2), which may be resulted from the partial blocking of the cavities in pure hierarchical TiO_2 by the modified Pd nanoparticles.

The optical absorption properties and visual changes of the hierarchical TiO_2 decorated with different amounts of Pd were demonstrated in Fig. 7a. All Pd-decorated TiO_2 have almost similar absorption intensity presented at UV wavelength due to the intrinsic absorption of pure anatase TiO_2. However, the introduction of Pd into pristine TiO_2 enhanced the absorption significantly and broadened the absorbance throughout the visible light range, accompanied with the color of the samples darkened from yellowish to dimgray as the Pd loading content increased to 2.5%. The high optical absorbance might be attributed by the Schottky heterojunctions formed on the interface between Pd and the TiO_2, which facilitated the charge transferring from the TiO_2 semiconductor to Pd cocatalyst. On the other side, the Surface Plasmon Resonance (SPR), resulted from the collective oscillation of the free conduction band electrons upon interaction with the incident electromagnetic radiation, might also partially contribute to the enhanced light absorption. But the plasmonic band of Pd was not observed in visible region due to its ultra-small particles size and low content [46]. The enhanced absorption capacity might be in favor of the light-harvesting efficiency and improving the photocatalytic activity. In Fig. 7b, a strong photoluminescence (PL) emission peak was observed for the pristine hierarchical TiO_2, owing to the high bulk recombination of charge carriers. The strong PL was quenched obviously as the Pd loading, and the lowest peak was achieved by the 1.5% Pd content. When the excessive dose of Pd was incorporated, the Pd would serve as defective sites to capture the photo-induced electrons to further generate excitons thus leading to the improvement of PL emission intensity.

Photocatalytic H_2 production experiments were performed using the catalysts of pristine hierarchical TiO_2 and the modified with various amounts of 0.5%, 1.0%, 1.5%, 2.0% and 2.5% Pd under UV–vis irradiation (λ = 320–780 nm) and simulated solar light (coupling with a cut-off filter of AM1.5G), respectively. As shown in Fig. 8, the pristine TiO_2 just displayed quite inappreciable rate of H_2 evolution under the condition. However, incorporating with Pd, the H_2 production rate could be remarkably improved. Similarly, upon increasing the Pd content in the composite catalyst, the rate of H_2 production exhibited the coincident trends of rising under both UV–vis and simulated solar light, respectively, achieved the maximum with the rates of 979.7 $\mu mol\ h^{-1}$ and 112.7 $\mu mol\ h^{-1}$, when the content of Pd was 1.5%. In addition, the 1.5% Pd/TiO_2 attained 120.9 turnover numbers (TON) and turnover frequency (TOF) of 40.3 h^{-1} after 3 h irradiation under simulated solar light (Supporting Information, Table S1). Nevertheless, further increasing the content of Pd in the hybrid has resulted in a gradual declined of the rate of H_2 evolution, which could be attributed to the excess amounts of Pd in Pd/TiO_2 caused much more surface defects, which would trap the photo-excited electrons thus gave rise to the decrease of photocatalytic activity. Comparatively,

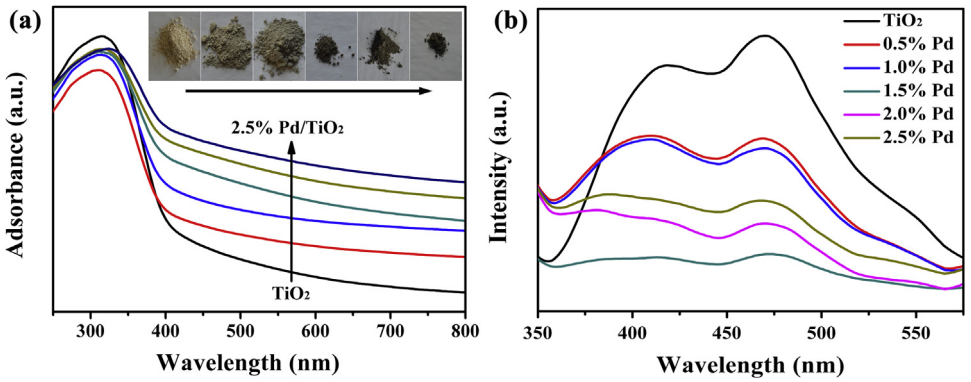

Fig. 7. UV–vis diffuse reflectance spectra of the prepared hierarchical TiO_2 and the decorated with various amounts of Pd (a) and the color change with the increase of Pd content (inset); (b) PL spectra of the various amounts of Pd decorated TiO_2.

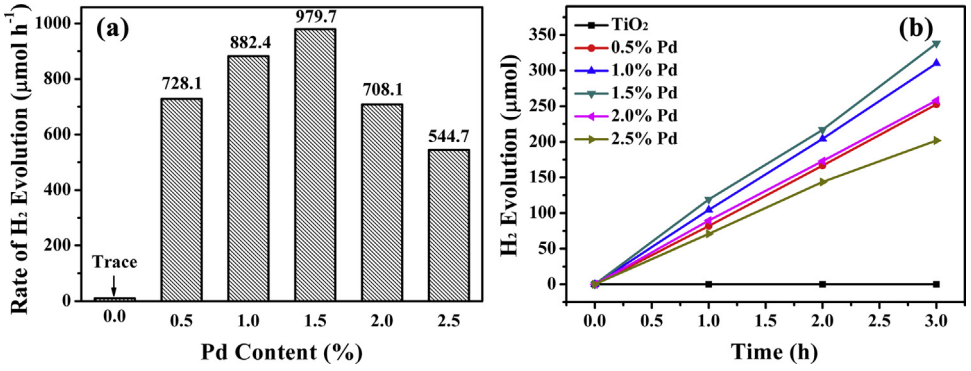

Fig. 8. Photocatalytic H_2 production over Pd/TiO_2 composite samples loading with varied amounts of Pd from 20 vol% methanol aqueous solution in total 3 h under varied light irradiation (a) under UV–vis light; (b) under simulated solar light.

the 1.5% Pd/NH_2-MIL-125(Ti) was synthesized and evaluated the photocatalytic H_2 activity under same conditions, but there are no perceptible H_2 produced (Fig. S6). Although the Pt/Ti-MOF-NH_2 could exhibit efficient photocatalytic activities for H_2 production by linker-to-cluster charge-transfer (LCCT) under visible light [32], the current 1.5% Pd/NH_2-MIL-125(Ti) is no activity for H_2 evolution, which may be resulted from the lower work function of Pd than Pt and the labile coordination bonds of NH_2-MIL-125(Ti) in aqueous solution [38]. What's more, to manifest the universality of such a MOF-constructed hierarchical TiO_2 in establishing of photocatalyst, and explore the effects of cocatalyst, the other noble metal such as Pt, Au and Ag modified hierarchical TiO_2 with identical content of 1.5% were prepared and employed to conduct the comparison of photocatalytic performance under simulated solar light. As exhibited in Fig. S5, the 1.5% Pd/TiO_2 possesses a competitive photocatalytic activity among listed other noble metal decorated the TiO_2 with 1.5%. In these metal/TiO_2 interfaces, a Schottky junction could be formed, which can accelerate charge separation. And the efficiency of charge separation is obviously dependent on the work function of the metal and the activation energy for H_2 production. On one hand, the work function of Pt and Pd are 5.65 eV and 5.12 eV, higher than Au (5.1 eV) and Ag (4.26 eV), that is, lower Fermi level and facilitate to trap electrons [47,48]. On the other hand, a "volcano plot" was exploited to elucidate the relationship between Gibbs free energy for atomic hydrogen adsorption (ΔG_H) and exchange current density. When the location of metal is closer to the peak of volcano, ΔG_H approaches zero, presenting higher activity for H_2 evolution. Pt and Pd are close and located near the peak of volcano, yet much higher than Au and Ag [49]. Thus, among the varied metal, Pt and Pd are the best candidate cocatalyst for H_2 evolution under current condition. Whereas, the loading amount

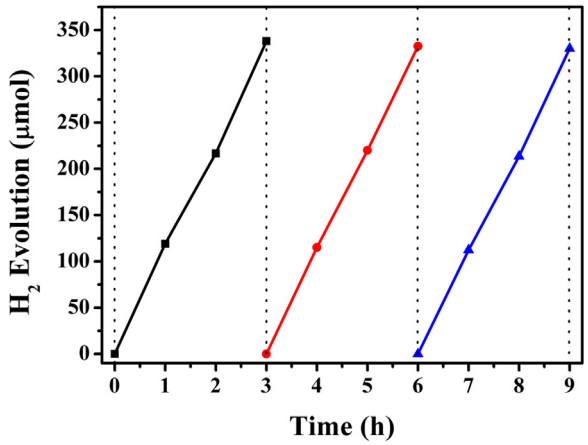

Fig. 9. Photo-stability study of photocatalytic H_2 evolution over the 1.5% Pd/TiO_2 under simulated solar light.

of a cocatalyst is the key point for the photocatalytic activity of the cocatalyst-loaded semiconductor photocatalyst. The optimal amounts of Pd may cause its activity higher than the Pt with equal amounts [50].

In addition, the photo-stability of the 1.5% Pd/TiO_2 was examined in three consecutive runs of total 9 h under simulated solar light. As demonstrated in Fig. 9, in each run, there were no noticeable deactivation occurred as the reaction proceeded. It illustrated the current hierarchical TiO_2 modified with 1.5% of Pd endowed distinguished stability for H_2 evolution under simulated solar light irradiation.

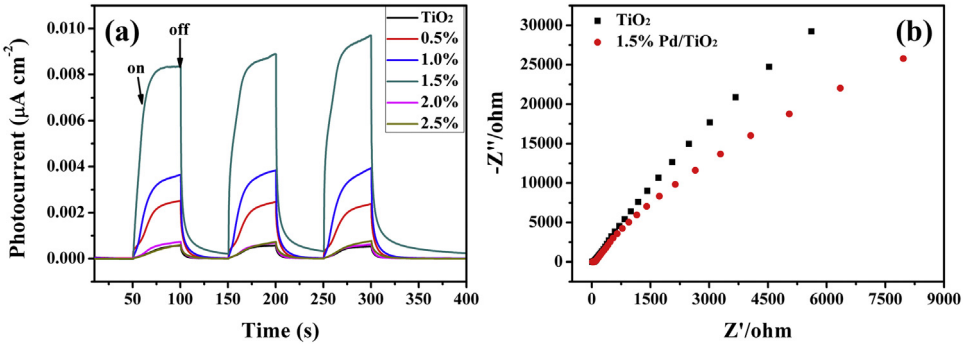

Fig. 10. (a) photocurrent response of the samples of decorated with various amounts of Pd; (b) EIS Nyquist plots of the pure hierarchical TiO_2 and 1.5% Pd/TiO_2.

To examine the difference of electronic interaction in the varied amounts of Pd decorated TiO_2, the photocurrent response and electrochemical impedance spectroscopy (EIS) were measured under the same condition (seen in Fig. 10). In the several intermittent "light on-off" cycles, the photocurrent value decreased to zero when the light irradiation was switched off and the photocurrent regained to a constant value as soon as the light was on, which was entirely reversible. Also, it could be visibly seen that the photocurrent response values exhibited an order of 1.5% Pd > 1.0% Pd > 0.5% Pd > 2.0% Pd > 2.5% Pd > pure TiO_2, the tendency was exactly coincident with the performance of H_2 evolution. At the same time, it also suggested the 1.5% content of Pd was optimum for efficient separation and transform of the photo-generated electron-hole pairs. Furthermore, the decreased electron-transfer resistance in 1.5% Pd/TiO_2 was confirmed by the EIS measurement, resulting from the smaller diameter of the semicircular Nyquist plots.

4. Conclusions

In summary, in order to expand the application of the MOFs-constructed hierarchical TiO_2 to photocatalytic field, we demonstrated a facile method to prepare a series of Pd decorated TiO_2 through the directly pyrolysis of Ti-containing MOFs of NH_2-MIL-125(Ti) precursors combined with photo-reduction process. The obtained hierarchical TiO_2 maintained the original rectangular submicron-tablet morphology of Ti-MOFs and was composed of small anatase TiO_2 nanoparticles. The hierarchical TiO_2 could be served as an ideal platform to load additional metal particles such as Pd, Pt, Au and Ag to achieve efficient photocatalysts. The Pd decorated TiO_2 exhibited considerably enhanced photocatalytic activity towards the H_2 evolution, ascribed from the improved optical absorption, efficient separation and migration of photo-induced electron-hole pairs. Particularly, the optimized 1.5% Pd/TiO_2 exhibited the highest rate of H_2 evolution of 979.7 $\mu mol\,h^{-1}$ and 112.7 $\mu mol\,h^{-1}$, under UV–vis light and simulated solar light, respectively. This work may provide a new efficient platform to construct metal or metal oxides modified hierarchical TiO_2 for efficient H_2 evolution under solar light and enlighten the design of other robust photocatalysts by the MOFs-templated transformation route.

Acknowledgments

We appreciate the financial support of the NSFC (U1503391) and International Cooperation Project of Xinjiang Science and Technology Bureau (2017E0116).

Appendix A. Supplementary data

Supplementary data associated with this article can be found, in the online version, at http://dx.doi.org/10.1016/j.apcatb.2017.07.020.

References

[1] Z. Han, R. Eisenberg, Acc. Chem. Res. 47 (2014) 2537–2544.
[2] P.D. Tran, L.H. Wong, J. Barber, J.S.C. Loo, Energy Environ. Sci. 5 (2012) 5902–5918.
[3] A. Fujishima, K. Honda, Nature 238 (1972) 37–38.
[4] R. Asahi, T. Morikawa, T. Ohwaki, K. Aoki, Y. Taga, Science 293 (2001) 269–271.
[5] T. Umebayashi, T. Yamaki, H. Itoh, K. Asai, J. Phys. Chem. Solids 63 (2002) 1909–1920.
[6] E. Grabowska, M. Marchelek, T. Klimczuk, G. Trykowski, A. Zaleska-Medynska, J. Mol. Catal. A: Chem. 423 (2016) 191–206.
[7] J. Yu, J. Ran, Energy Environ. Sci. 4 (2011) 1364–1371.
[8] Y. Ma, X. Wang, Y. Jia, X. Chen, H. Han, C. Li, Chem. Rev. 114 (2014) 9987–10043.
[9] X. Li, J. Yu, J. Low, Y. Fang, J. Xiao, X. Chen, J. Mater. A 3 (2015) 2485–2534.
[10] M. Gao, L. Zhu, L.O. Wei, J. Wang, G.W. Ho, Catal. Sci. Technol. 5 (2015) 4703–4726.
[11] Z. Haider, Y.S. Kang, ACS Appl. Mater. Interfaces 6 (2014) 10342–10352.
[12] B. Zhu, K. Li, J. Zhou, S. Wang, S. Zhang, S. Wu, W. Huang, Catal. Commun. 9 (2008) 2323–2326.
[13] Z. Zhong, Y. Yin, B. Gates, Y. Xia, Adv. Mater. 12 (2000) 206–209.
[14] Z. Zheng, B. Huang, X. Qin, X. Zhang, Y. Dai, Chem. – Eur. J. 16 (2010) 11266–11270.
[15] T.R. Cook, Y.R. Zheng, P.J. Stang, Chem. Rev. 113 (2013) 734–777.
[16] J.R. Li, J. Sculley, H.C. Zhou, Chem. Rev. 112 (2012) 869–932.
[17] J.R. Li, R.J. Kuppler, H.C. Zhou, Chem. Soc. Rev. 38 (2009) 1477–1504.
[18] D. Farrusseng, S. Aguado, C. Pinel, Angew. Chem. Int. Ed. 48 (2009) 7502–7513.
[19] L.E. Kreno, K. Leong, O.K. Farha, M. Allendorf, R.P. Van Duyne, J.T. Hupp, Chem. Rev. 112 (2012) 1105–1125.
[20] S.L. Li, Q. Xu, Energy Environ. Sci. 6 (2013) 1656–1683.
[21] B. Liu, H. Shioyama, T. Akita, Q. Xu, J. Am. Chem. Soc. 130 (2008) 5390–5391.
[22] T. Zhang, W. Lin, Chem. Soc. Rev. 43 (2014) 5982–5993.
[23] L. Zhang, H.B. Wu, X.W. Lou, J. Am. Chem. Soc. 135 (2013) 10664–10672.
[24] L. Zhang, H.B. Wu, S. Madhavi, H.H. Hng, X.W. Lou, J. Am. Chem. Soc. 134 (2012) 17388–17391.
[25] S. Furukawa, J. Reboul, S. Diring, K. Sumida, S. Kitagawa, Chem. Soc. Rev. 43 (2014) 5700–5734.
[26] K.E. deKrafft, C. Wang, W. Lin, Adv. Mater. 24 (2012) 2014–2018.
[27] X. Cao, B. Zheng, X. Rui, W. Shi, Q. Yan, H. Zhang, Angew. Chem. Int. Ed. 53 (2014) 1404–1409.
[28] C.H. Hendon, D. Tiana, M. Fontecave, C. Sanchez, L. D'Arras, C. Sassoye, L. Rozes, C. Mellot-Draznieks, A. Walsh, J. Am. Chem. Soc. 135 (2013) 10942–10945.
[29] L. Huang, B. Liu, RSC Adv. 6 (2016) 17873–17879.
[30] S.R. Zhu, P.F. Liu, M.K. Wu, W.N. Zhao, G.C. Li, K. Tao, F.Y. Yi, L. Han, Dalton Trans. 45 (2016) 17521–17529.
[31] T. Toyao, M. Saito, H. Yu, K. Mochizuki, M. Iwata, H. Higashimura, M. Matsuoka, Catal. Sci. Technol. 3 (2013) 2092–2097.
[32] H. Yu, T. Toyao, M. Saito, K. Mochizuki, M. Iwata, H. Higashimura, M. Anpo, M. Matsuoka, J. Phys. Chem. C 116 (2012) 20848–20853.
[33] Y. Fu, D. Sun, Y. Chen, R. Huang, Z. Ding, X. Fu, Z. Li, Angew. Chem. Int. Ed. 51 (2012) 3364–3367.
[34] Z. Xiu, M.H. Alfaruqi, J. Gim, J. Song, S. Kim, T.V. Thi, P.T. Duong, J.P. Baboo, V. Mathew, J. Kim, Chem. Commun. 51 (2015) 12274–12277.
[35] Z. Wang, X. Li, H. Xu, Y. Yang, Y. Cui, H. Pan, Z. Wang, B. Chen, G. Qian, J. Mater. Chem. A 2 (2014) 12571–12575.
[36] P. Wang, J. Lang, D. Liu, X. Yan, Chem. Commun. 51 (2015) 11370–11373.
[37] J. Dou, Y. Li, F. Xie, X. Ding, M. Wei, Cryst. Growth Des. (2015) 49–50.

[38] Z. Guo, J. Cheng, Z. Hu, M. Zhang, Q. Xu, Z. Kang, D. Zhao, RSC Adv. 4 (2014) 34221–34225.
[39] K. Khaletskaya, A. Pougin, R. Medishetty, C. Rösler, C. Wiktor, J. Strunk, R.A. Fischer, Chem. Mater. 27 (2015) 7248–7257.
[40] X. Chen, X. Wang, X. Fu, Energy Environ. Sci. 2 (2009) 872–877.
[41] Q. Xiang, J. Yu, M. Jaroniec, J. Am. Chem. Soc. 134 (2012) 6575–6578.
[42] Z.H.N. Al-Azri, W.T. Chen, A. Chan, V. Jovic, T. Ina, H. Idriss, G.I.N. Waterhouse, J. Catal. 329 (2015) 355–367.
[43] V. Jovic, P.H. Hsieh, W.T. Chen, D.S. Waterhouse, T. Söhnel, G.I.N. Waterhouse, Int. J. Nanotechnol. 11 (2013) 686–694.
[44] M. Danhardi, C. Serre, T. Frot, L. Rozes, G. Maurin, C. Sanchez, G. Férey, J. Am. Chem. Soc. 131 (2009) 10857–10859.
[45] Y. Fu, L. Sun, H. Yang, L. Xu, F. Zhang, W. Zhu, Appl. Catal B 187 (2016) 212–217.
[46] Y. Chang, J. Xu, Y. Zhang, S. Ma, L. Xin, L. Zhu, C. Xu, J. Phys. Chem. C 113 (2009) 18761–18767.
[47] J. Yang, D. Wang, H. Han, C. Li, Acc. Chem. Res. 46 (2013) 1900–1909.
[48] X. Zong, H. Yan, G. Wu, G. Ma, F. Wen, L. Wang, C. Li, J. Am. Chem. Soc. 130 (2008) 7176–7177.
[49] T.F. Jaramillo, K.P. Jørgensen, J. Bonde, J.H. Nielsen, S. Horch, I. Chorkendorff, Science 317 (2007) 100–102.
[50] J. Ran, J. Zhang, J. Yu, M. Jaroniec, S.Z. Qiao, Chem. Soc. Rev. 43 (2014) 7787–7812.